Journal of Catalysis **195,** 383–393 (2000)
doi:10.1006/jcat.2000.2998, available online at http://www.idealibrary.com on IDEAL®

New PtRu Alloy Colloids as Precursors for Fuel Cell Catalysts

U. A. Paulus,*,[1] U. Endruschat,† G. J. Feldmeyer,* T. J. Schmidt,*,[2] H. Bönnemann,† and R. J. Behm*

*Abt. Oberflächenchemie und Katalyse, Universität Ulm, D-89069 Ulm, Germany; and †Max-Planck-Institut für Kohlenforschung, D-45470 Mülheim, Germany

Received April 25, 2000; revised July 11, 2000; accepted July 11, 2000

We describe the preparation and characterization of new PtRu alloy colloids that are suitable as precursors for fuel cell catalysts. The new, simplified preparation method, which uses an organometallic compound both for reduction and as colloid stabilizer, leads to a PtRu colloid possessing lipophilic surfactant stabilizers. These can easily be modified to show hydrophilic properties. Prior to electrochemical measurements the surfactant shell is removed by reactive annealing in O_2 and H_2. Comparing the electrocatalytical activity of the Vulcan-supported colloids with that of a differently prepared PtRu colloid investigated recently and with a commercially available PtRu catalyst, we found practically identical activities with respect to CO and CO/H_2 oxidation. Activities of similar order of magnitude were found also for methanol oxidation. The results demonstrate the high potential of the new, organometallic preparation scheme for the synthesis of colloid precursors for bimetallic catalysts, especially if it is considered that variations in the alloy composition can easily be realized using the colloidal preparation method.

Key Words: **PtRu colloids; fuel cell catalysts; thin-film electrodes; rotating disk electrode.**

1. INTRODUCTION

Supported metal catalysts, both for heterogeneous (chemical) catalysis and for electrocatalysis, are prepared by various methods, e.g., impregnation, coprecipitation, etc. In practically all of these schemes the active metal particles are formed by *in situ* reduction from a metal salt on the catalyst. An alternative route, involving the use of prefabricated small metal particles that are subsequently deposited on the respective support material, has found little technical application so far. Reasons for that include, e.g., problems associated with the particle preparation and, even more important, with keeping the small particles separated. Some years ago several groups proposed to avoid the latter problem by stabilizing the metal particles with organic molecules, which prevent agglomeration and coalescence of the particles (1–6). If necessary the stabilizer shell is removed after the colloid particles are fixed on the respective support. The use of stabilized metal particles as catalyst precursors appears to be especially attractive for the preparation of bimetallic or even multicomponent catalysts, since in addition to other advantages the particle composition can be controlled rather well during synthesis. The possibility to produce bimetallic catalysts with small particles and a narrow size distribution, even at high metal loading, and a defined particle composition makes this synthesis scheme very interesting for reactions which operate at not too high temperatures, so that the initial particle sizes and composition will largely be maintained during reaction.

One potential application for catalysts prepared from stabilized colloid precursors is in low-temperature fuel cells, in hydrogen-operated polymer electrolyte membrane fuel cells (PEM-FC), as well as in methanol-operated direct methanol fuel cells (DMFC). In these fuel cells Pt alloys, most importantly PtRu alloys, are known to be the most active and CO tolerant anode catalysts for the oxidation of CO-contaminated H_2 (e.g., H_2 obtained from methanol or gas reformation) in PEM-FCs (7, 8), a significant activity enhancement was found also in DMFC as compared to pure Pt anode catalyst (9, 10). The successful application of tenside stabilized PtRu particles as catalyst precursors for PEM-FC anode catalysts was recently demonstrated by our group (11–13) and subsequently also by other groups (14). For this purpose high-area fuel cell catalysts with well-defined, completely alloyed bimetallic particles and a narrow particle size distribution with less than 3 nm diameter were prepared by adsorbing surfactant-stabilized preformed PtRu colloids on high-surface-area Vulcan XC72 (12). We first developed a conditioning procedure for the Vulcan-supported colloid in order to quantitatively remove the stabilizer, $N(oct)_4Cl$ (12), and characterized the electrocatalytic properties of a $Pt_{0.5}Ru_{0.5}$ colloid supported on glassy carbon (11), then we investigated the electrocatalytical activity of the conditioned Vulcan-supported catalyst with respect to CO/H_2 oxidation (12) and methanol electrooxidation (13). The results showed that without any

[1] To whom correspondence should be addressed. Present address: Paul Scherrer Institut, Forschungsbereich Allgemeine Energieforschung, CH-5232 Villigen PSI, Switzerland. Fax: +41-56-310-4415. E-mail: ursula.paulus@psi.ch.

[2] Present address: Lawrence Berkeley National Laboratory, Materials Science Division, University of California, Berkeley, CA 94720.

0021-9517/00 $35.00

further optimization the activity and CO tolerance of these catalysts were practically identical with those of state-of-the-art commercial catalysts (E-TEK).

Despite the very promising results the application of these colloid-based catalysts is still hindered or even inhibited by the complex colloid synthesis and catalyst preparation, leading to a noncompetitive catalyst price. We here report on a new colloid-based PtRu catalyst, where the colloid precursor is prepared along a novel simplified route, by using organoaluminum molecules for both coreduction of the Pt and Ru salts and for stabilizing the resulting PtRu colloid particles. Although this route is still very complex compared to the commercially used coimpregnation method it has some advantages that may be of interest for further catalyst development and improvement. This synthesis scheme avoids the use of chloride-containing stabilizers. The further handling of the colloids can also be simplified by converting the hydrophobic colloids into a more hydrophilic form dissolvable in aqueous solutions, which is achieved by modification of the alkane end groups into alkoxy groups.

In this report we will concentrate on the preparation and the physical and electrochemical characterization of the carbon (Vulcan XC72)-supported PtRu catalyst as well as on the evaluation of the electrocatalytical properties; the synthesis of the colloid particles is described in more detail in Ref. (15). Following a brief description of the experimental details and procedures, including the colloid synthesis, the catalyst preparation, and the electrochemical procedures, we will first describe the optimization of the conditioning procedure to remove the stabilizer molecules. The decomposition of the stabilizing shell and the particle composition was followed at the different stages of the conditioning procedure by X-ray photoelectron spectroscopy (XPS). For the optimized procedure the particle size/particle size distribution was determined by high-resolution transmission electron microscopy (HRTEM) at the different stages of the procedure, i.e., for the unsupported "raw" colloid, for the Vulcan-supported colloid, and for the Vulcan-supported catalyst after conditioning, which allows us to quantify the effect of temperature-induced sintering of the alloys. In addition, the particle composition was controlled by energy dispersive X-ray analysis (EDX). In the next section the electrochemical properties and the catalytic activity of the Vulcan-supported catalyst are characterized by CO stripping voltammetry. The final sections deal with the electrocatalytic activity and behavior of the supported PtRu catalysts under fuel cell relevant conditions (pseudo-steady-state oxidation of reactants at 60°C), using the thin-film rotating disk method (RDE) developed recently in our group (16). This enables us to quantify the electrocatalytic activity under well-defined mass-transport conditions and with complete catalyst utilization. The current densities determined in our RDE measurements can be correlated with the performance data obtained for full cells on the basis of mass-specific current densities, allowing predictions on the kinetic limit of their performance, in the absence of transport limitations and ohmic resistances (12, 17). Reactions investigated include the continuous oxidation of 2% CO/H_2 (simulated reformer gas), the potentiostatic oxidation of more diluted CO/H_2 mixtures in order to evaluate the CO tolerance of these catalysts for comparison with real PEM single-cell data, and the potentiostatic oxidation of methanol for comparison with DMFC data.

For all reactions both the unmodified and modified PtRu catalysts obtained via organoaluminum reduction were investigated. To quantify effects caused by the new colloid synthesis procedure and to assess the activity of the colloid-based PtRu catalysts as compared to state-of-the-art commercial PtRu catalysts prepared by traditional schemes, we compare with similar data recorded for the Vulcan-supported PtRu catalyst obtained from the $Pt_{0.5}Ru_{0.5}N(oct)_4Cl$ precursors, and for commercial Vulcan-supported PtRu catalysts (E-TEK). The data demonstrate that the new simplified route for colloid synthesis produces highly active PEM-FC and DMFC anode catalysts with a narrow particle size distribution.

2. EXPERIMENTAL

2.1. Catalyst Preparation and Characterization

The organometallic preparation of the bimetallic PtRu colloids follows the reaction described in Eq. [1] (acac = acetylacetonate):

$$Pt(acac)_2 + Ru(acac)_3 + 8Al(me)_3 \rightarrow PtRu_{colloid} + [R_2Al(acac)]. \quad [1]$$

A detailed description of the synthesis procedure is given in Ref. (15). In short, a solution of the reducing agent $Al(CH_3)_3$ (1.20 g = 16 mmol of $Al(CH_3)_3$ dissolved in 50 ml of toluene) is slowly added over 4 h to the vigorously stirred and slightly warmed (40°C) solution of the two metal salts (0.79 g = 2 mmol of $Pt(acac)_2$ and 0.80 g = 2 mmol of $Ru(acac)_3$, dissolved under an argon atmosphere in 150 ml of dry toluene). To complete the reaction the mixture is stirred for additional 20 h. The dark red color of the solution slowly changes with time to black. To remove any precipitate the reaction solution is filtered. Subsequently all volatile components are completely evaporated in vacuum (10^{-3} mbar, 40°C, 16 h). The elemental analysis shows metal contents of 13.2 wt% Pt and 6.8 wt% Ru, corresponding to a 1 : 1 ratio of Pt to Ru.

The colloids prepared in this way still have Al–CH_3 functions in the protecting shell which lead to a hydrophobic behavior. To obtain more hydrophilic characteristics the organic stabilizers can be modified as shown in the scheme in Fig. 1.

For this a solution of 0.5 g of Brij 35 (polyethylenglycol–dodecylether) dissolved in 50 ml of dry toluene is dropped

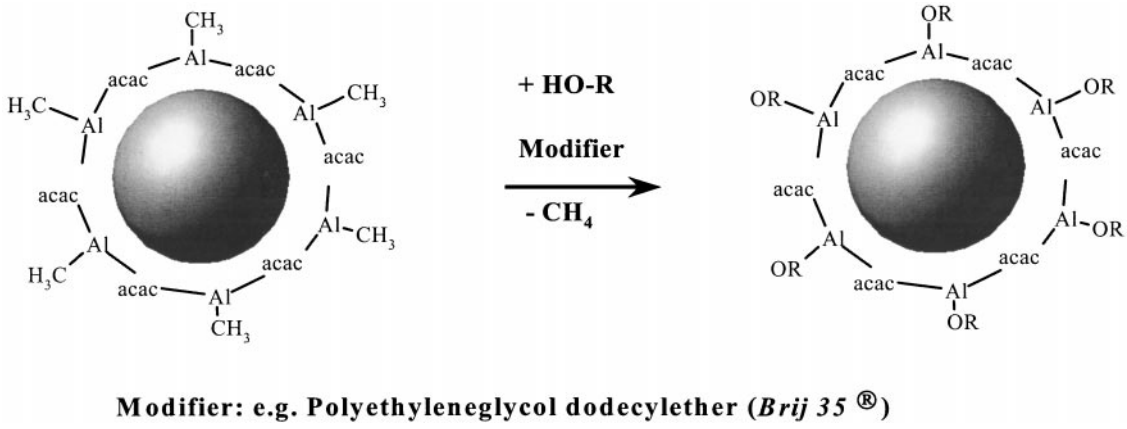

FIG. 1. Reaction scheme presenting the modification of colloids which still have Al–CH_3 functions in their protecting shell.

to a solution of 0.7 g of the freshly prepared bimetallic PtRu colloid. The substitution of the methyl groups by alkoxides is accompanied by methane evolution. Elemental analysis of the product shows metal contents of 6.5 wt% Pt and 3.7 wt% Ru, still corresponding to a 1 : 1 ratio of the two metals. The modified bimetallic colloid is soluble in hydrophobic and hydrophilic solvents including water.

For the XPS characterization of the conditioning procedure the colloids were supported on a planar α-quartz $[01\bar{1}0]$ substrate. For this 20 μl of clear colloid dispersion, prepared from a dispersion of 0.1 mg/l colloid in dry tetrahydrofuran (THF, Merck, p.a.) by stirring in an ultrasonic bath, was pipetted onto the preannealed α-quartz $[01\bar{1}0]$ surface. After evaporation of the solvent film the crystal was transferred into a UHV chamber (2×10^{-10} mbar). Reactive annealing steps for removal of the stabilizer shell (each for 30 min at the respective temperature) were carried out in UHV, in O_2 (Linde N4.5) and in H_2 (Linde N5.0), respectively.

For electrochemical measurements the organoaluminum colloids were supported on high-surface-area carbon (PtRu colloid unmodified and PtRu colloid modified/Vulcan XC72, 20 wt% metal content) by dropping a colloid dispersion in toluene (unmodified, 1.09 g/100 ml; modified, 3.68 g/ 100 ml) to a suspension of Vulcan in the same solvent (1.06 g/100 ml). The Vulcan suspension was heated to 40°C under vigorous stirring before the colloid dispersion was added. After being stirred for another 24 h the remaining solution was decolorized. The solvent was evaporated and the catalyst was rinsed with pentane. Finally the catalyst powder was dried at room temperature.

The Vulcan-supported dried catalyst powders were conditioned in a tube furnace prior to the electrochemical measurements, submitting it to the same conditioning procedure developed for the planar substrates under XPS control. The conditioning procedure involves two reactive annealing steps, heating the powder first in an air/Ar mixture (scientific grade, Messer Griesheim/Westfalen N6.0) and then in pure hydrogen (Westfalen N5.0) for 30 min each to completely remove the surfactant stabilizer. The particle size distribution and the dispersion, D, resulting after this conditioning procedure were determined by high-resolution transmission electron microscopy (HRTEM). Table 1 gives an overview of the physical properties of the

TABLE 1

Comparison of the Particle Size and Composition of the Different PtRu Colloid Precursors (Rows 2 and 3) and of the Resulting Catalysts (Rows 4 to 6)

Colloid/resulting catalyst	Composition (according to EDX)	Mean particle diameter $\bar{d}$ (nm)	Dispersion D (%)
Raw PtRu(AlR_3) colloid, unmodified	$Pt_{0.5}Ru_{0.5}$	1.2 ± 0.3	78
Raw PtRu(AlR_3) colloid, modified	$Pt_{0.48}Ru_{0.52}$	1.4 ± 0.3	69
PtRu(AlR_3)/Vulcan, unmodified	$Pt_{0.52}Ru_{0.48}$	Unconditioned: 1.3 ± 0.4	67
		Conditioned: 1.5 ± 0.4	58
PtRu(AlR_3)/Vulcan, modified	$Pt_{0.53}Ru_{0.47}$	Unconditioned: 1.5 ± 0.4	60
		Conditioned: 1.8 ± 0.5	50
PtRu(NR_4)/Vulcan	$Pt_{0.52}Ru_{0.48}$ (12)	Conditioned: 2.3 ± 0.5 (12)	43 (12)
PtRu/Vulcan (E-TEK)	$Pt_{0.50}Ru_{0.50}$	Conditioned: 2.1 ± 0.3 (26)	44 (26)

Note. Data for the commercially available PtRu/Vulcan catalyst (E-TEK) are provided as a reference.

colloids considered in this presentation. In order to avoid any misunderstanding in the following text, the resulting catalysts (i.e., the Vulcan-supported and conditioned catalysts) are referred to as "PtRu(AlR_3)/Vulcan, unmodified" (before conversion into a hydrosol), "PtRu(AlR_3)/Vulcan, modified" (after conversion into a hydrosol), and "PtRu(NR_4)/Vulcan" for the catalyst obtained from the $Pt_{0.5}Ru_{0.5}N(oct)_4Cl$ precursors. Accordingly, the respective colloid precursors will be denoted as PtRu(AlR_3) and PtRu(NR_4).

2.2. Electrode Preparation and Electrochemical Measurements

The electrochemical measurements were conducted in a thermostated standard three-compartment electrochemical cell using an interchangeable rotating disk electrode setup (Pine Instruments). Potentials were measured using a saturated calomel electrode (SCE) separated from the working electrode compartment by a closed electrolyte bridge in order to prevent chloride contamination of the electrolyte. The potentials in this study, however, all refer to that of the reversible hydrogen electrode (RHE).

The electrodes were prepared as described by Schmidt *et al.* (12, 16). In short, aqueous suspensions (Millipore water) containing 0.5 mg/ml conditioned Vulcan-supported catalyst were obtained by ultrasonic mixing for about 15 min. Glassy carbon disk electrodes (6 mm diameter, 0.283 cm^2, Sigradur G, Hochtemperaturwerkstoffe GmbH) served as substrate for the catalyst powder. They were polished to a mirror finish (0.05 μm alumina, Buehler) prior to each experiment. A 20-μl volume of the catalyst suspension was pipetted onto the carbon substrate, resulting in a noble metal loading of 7 μg of metal/cm^2. After evaporation of the water in a mild argon stream, 20 μl of a dilute Nafion solution (prepared similar as described in Ref. (18)) was pipetted onto the electrode surface in order to fix the catalyst particles onto the glassy carbon surface after evaporation of the solvent, resulting in a Nafion film thickness of $\sim$0.2 μm. For methanol electrooxidation electrodes with 14 μg of metal/cm^2 were used. Previous studies had shown that film diffusion effects are negligible under these conditions (16).

Directly after preparation the electrodes were immersed into the Ar-purged electrolyte (0.5 M H_2SO_4, Merck suprapure) under potential control at 0.1 V. Owing to the clean preparation procedure, no further pretreatment (e.g., potential cycling) was necessary. The positive potential applied to PtRu/Vulcan electrodes was limited to 0.75 to 0.8 V RHE in order to avoid Ru dissolution. For CO stripping voltammetry, CO (Messer-Griesheim N4.7) was adsorbed onto the electrode surface at 0.1 V for 3 min at a rotation rate of 900 rpm. Subsequently the electrolyte was purged with argon for 15 min before the stripping peak was measured. Prior to continuous oxidation of CO in H_2 (Messer-Griesheim N4.7/N5.0) the electrode surface was equilibrated with the gas-saturated electrolyte at 0.05 V for 15 min at 2% CO/H_2 and at 0.015 V for up to 3 h in the case of more diluted CO concentrations (prepared by electronic mass flow controllers, MKS, $\pm$0.8% full scale).

For the methanol oxidation measurements the electrodes were held at 0.05 V and methanol (Merck, p.A.) was injected to reach a methanol concentration of 0.5 or 2.0 mol/l. After an additional 3 min at this potential the electrodes were stepped to potentials between 0.4 and 0.55 V. At each potential the electrodes were held for 30 min to simulate steady-state conditions. One data set was always recorded with a single sample, i.e., after stepping from 0.05 to 0.4 V the next step to 0.45 V was performed.

3. RESULTS AND DISCUSSION

3.1. Physical Characterization of the Catalysts by XPS and TEM

The decomposition and quantitative removal of the stabilizer molecules was followed by XP spectroscopy. For these measurements both the modified and the unmodified unsupported PtRu colloids were adsorbed onto an atomically smooth α-quartz [0110] substrate as described in the previous section and transferred into the UHV chamber. We used α-quartz instead of chemically more appropriate graphite (HOPG) substrates, since on the latter substrates the Ru(3*d*) signal of the colloid and the C(1*s*) signal of the stabilizer would be covered by the dominant C(1*s*) signal of the HOPG substrate. We were able to demonstrate (data not shown) that the temperature dependence of the decomposition process is identical (comparing the resulting particle composition) when α-quartz is used instead of HOPG. Because of the superimposition between the Al(2*p*) signal (stabilizer) and the Pt(4*f*) signal (colloid) the latter signal was not accessible for following the stabilizer decomposition, as had been done when investigating the conditioning procedure for the PtRu(NR_4)/Vulcan catalyst (12). Therefore, we refer to the Ru(3*d*) and the Pt(4*d*) signals when discussing the conditioning procedure.

The change in composition of the colloid particles and their organic shell after the different processing steps is demonstrated in the XP spectra in Fig. 2 for both the unmodified (2A) and the modified PtRu(AlR_3)/Vulcan catalysts (2B). C(1*s*)/Ru(3*d*) and Pt(4*d*) spectra recorded directly after the transfer into the UHV chamber are shown first (curves a). In both cases the Ru(3*d*) signal is completely covered and obscured by an intense C(1*s*) signal, which according to its binding energy of 284.6 eV results from aliphatic carbon, i.e., from the stabilizer molecules. The very low intensity in the Pt(4*d*) signal indicates that the colloid particles are still completely covered by the stabilizer shell, which absorbs most of the electrons emitted from the metal

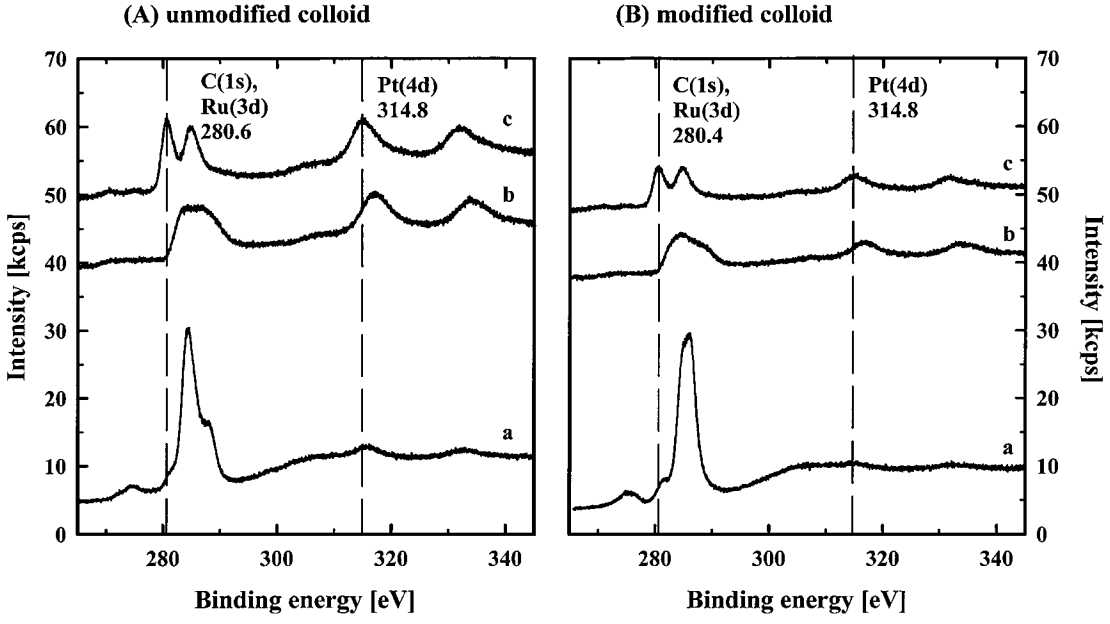

FIG. 2. XPS signals of the (A) unmodified and (B) modified PtRu colloid adsorbed on α-quartz [01$\bar{1}$0] before and after the applied conditioning steps: (a) adsorbed PtRu colloid (including the Al–organic stabilizer); (b) after oxidative annealing at 250°C (unmodified) and 300°C (modified); and (c) after reductive annealing at 250°C (unmodified) and 300°C (modified).

nucleus. Annealing cycles in 100 mbar O_2 (30 min) and subsequently in 50 mbar H_2 (30 min) at increasingly higher temperatures (200–300°C) showed that the organic stabilizer shell is practically completely removed after reactive annealing at 250°C for the unmodified colloid and at 300°C for the modified colloid. This is demonstrated in curves b and c, which were recorded after oxidation and reduction, respectively, under these conditions. The pronounced growth in intensity in the Pt(4*d*) together with an intensity decrease and broadening of the C(1*s*)/Ru(3*d*) signal indicates already that most or all of the organic shell is removed. Furthermore, from the binding energies (BEs) and width of both the Ru(3*d*) and the Pt(4*d*) signals of 283.6/3.3 eV and 316.9/5.9 eV, respectively, we can conclude that the noble metals are partially oxidized (the values are given for the unmodified colloid after 250°C treatment; those for the modified one are practically identical). The final reduction step in hydrogen (50 mbar, 30 min, curve c) shows only a little further increase in the Pt(4*d*) intensity. More important is the finding that for both colloids no C(1*s*) signal can be detected, neither by direct observation nor after deconvolution. The BEs/FWHMs of both the Ru(3*d*) signal (280.6/ 2.5 eV) and the Pt(4*d*) signal (314.8/5.5 eV) are typical of zero-valent noble metals. For both colloids Al is still present in the catalyst in partially oxidized form after the conditioning procedure. The influence of the remaining Al is up to now unclear and needs further investigation. However, it seems that the influence of Al on the electrocatalytical properties of the catalysts is negligible, if any. Finally it should be noted that comparative XPS measurements on graphite (HOPG)-supported PtRu(AlR_3) colloids showed no indications of oxidic noble metal species or aliphatic carbon after conditioning under the conditions determined for quartz supported colloids, indicating that the conditioning procedure/conditions are adequate also for the carbon-supported disperse catalysts.

In addition to the XPS characterization of the accessible particle surface, particle size distribution, dispersion, and composition of the catalyst particles were determined via HRTEM and EDX measurements for Vulcan-supported colloids before and after conditioning. The results obtained are listed in Table 1. For comparison the physical properties of the Vulcan-supported $N(oct)_4Cl$-stabilized PtRu colloid are included as well. The EDX measurements showed in all cases Pt/Ru ratios close to 1 for the individual particles. In contrast to the close similarity in particle compositions, the particle sizes of the AlR_3-stabilized and the NR_4-stabilized colloids and the resulting catalysts are quite different. The modified PtRu(AlR_3) colloid particles are about 15% larger than the unmodified ones, with a particle size distribution reaching from about 0.6 to 3.0 nm diameter in both cases. Adsorption on the Vulcan support leaves the particle sizes and size distributions practically unaffected (changes $\leq$10%). The conditioning procedure causes some temperature-induced sintering of the particles, which, as is obvious from the particle size distribution (compare Ref. (15)) and the particle size data in Table 1, is in both cases of the same order of magnitude (20%). Both the modified and the unmodified conditioned PtRu(AlR_3)/Vulcan catalyst particles are on average about 20 to 30% smaller

than the PtRu particles in the conditioned $PtRu(NR_4)$/Vulcan catalyst, underlining the role of the colloid synthesis procedure. Furthermore, the results also demonstrate that the smaller particle size reached by the newly developed method for colloid preparation is not compensated or even overcompensated by sintering effects during the necessary removal of the stabilizer shell, making this an indeed attractive route for producing bimetal catalysts.

3.2. CO Stripping Voltammetry at Room Temperature

To determine the active surface area of the catalyst particles after conditioning and to obtain further (indirect) information on their surface composition we characterized them by CO stripping experiments. The resulting stripping (solid line) and base voltammograms (dashed line) are shown in Fig. 3. The curves were recorded at 20 mV/s in 0.5 M H_2SO_4 at room temperature for (a) the unmodified $PtRu(AlR_3)$/Vulcan, (b) the modified $PtRu(AlR_3)$/Vulcan, and (c), for comparison, for the $PtRu(NR_4)$/Vulcan catalyst. First we realized that the maximum electrode potential which can be applied to the electrode without modifying it, as evidenced by a change in voltammograms recorded subsequently, is 0.75 V. This is slightly lower than the critical potential of 0.80 V reported for the $PtRu(NR_4)$/Vulcan catalyst. When higher potentials are applied, irreversible changes in catalyst composition take place due to the dissolution of Ru. For pure Ru this is known to take place at ≈0.9 V (19). In PtRu bulk alloys Gasteiger *et al.* (20) could show that an alloy with a surface Ru concentration of $x_{Ru,s} = 0.46$ is stable up to 0.95 V for a few cycles. The shift to lower values for the critical potential for Ru dissolution in our measurements is tentatively attributed to particle size effects. Accordingly this value is slightly lower for the smaller particles of the modified and unmodified $PtRu(AlR_3)$/Vulcan catalysts (mean particle diameters 1.5 and 1.8 nm, respectively) than for the $PtRu(NR_4)$Vulcan with a mean particle diameter of 2.3 nm. In both cases the critical potential for dissolution is significantly lower than for massive bulk samples.

The stripping peak potentials (peak maximum) of the unmodified and the modified $PtRu(AlR_3)$/Vulcan are nearly identical (0.66 and 0.63 V) within the experimental error of ±10 mV. These stripping peak potentials are significantly more negative than those obtained on pure Pt (20) or Pt/Vulcan (12) (≈0.8 V). They are, however, also distinctly more positive than the 0.57 V measured for the $PtRu(NR_4)$/Vulcan catalyst (12) or the 0.5 V determined for a bulk PtRu alloy with a surface composition of 50 atom% Ru (20). This negative shift of the peak compared to the peak of the Pt catalyst occurs due to the higher affinity of Ru for H_2O or OH species than of Pt. Therefore, CO adsorbed onto the electrode surface can be oxidized into CO_2 at lower potentials (20, 21). The more positive peak potential compared to that of the $PtRu(NR_4)$/Vulcan and a bulk

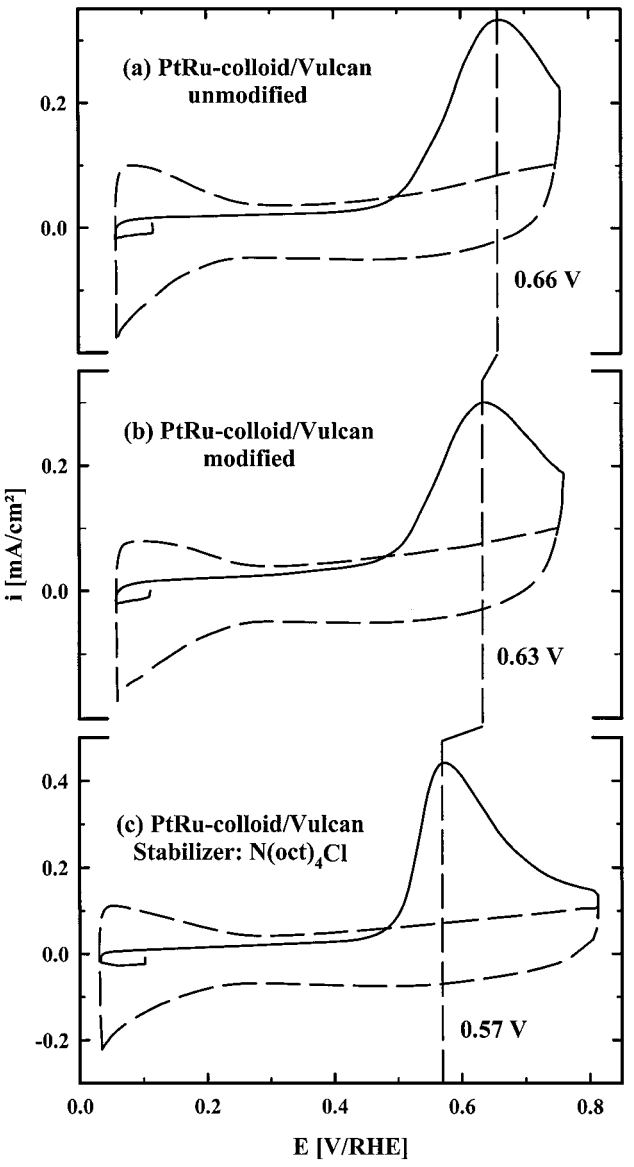

FIG. 3. Base voltammetry (---) and CO stripping (—) (20 mV/s) in 0.5 M H_2SO_4 at 25°C on high-surface-area electrodes with a metal loading of 7 $\mu g/cm^2$: (a) unmodified PtRu colloid/Vulcan, (b) modified PtRu colloid/Vulcan, and (c) PtRu colloid/Vulcan from the $N(oct)_4Cl$-stabilized precursor.

alloy with the surface composition of Pt : Ru = 1 : 1 may result from a surface enrichment in Pt, as reported in Ref. (20) for bulk alloys, but recent studies on supported catalysts found similar effects for decreasing particle sizes (22). Because of the practically similar conditioning procedure for the $PtRu(NR_4)$/Vulcan and the $PtRu(AlR_3)$/Vulcan catalysts we favor the latter explanation, attributing the anodic shift in the peak maximum to the smaller particle size in the latter catalyst. Further support for this model comes from the fact that at a particle diameter of 1.5 nm a surface enrichment in Pt sufficient to explain the shift would

require a significant depletion of the particle core; i.e., it would require a pronounced phase separation, which does not appear to be very likely. Finally it should be noted that different from the difference in peak position the onset of the stripping peaks for the three colloid-based PtRu catalysts occurs at almost identical potentials, which will be important for the understanding of the continuous oxidation of CO/H_2 mixtures described below.

Comparing the stripping peak area (each corrected for the capacitance of the carbon support) the charges of 1.78 mC/cm^2 obtained for the unmodified and 1.85 mC/cm^2 for the modified $PtRu(AlR_3)$ catalyst, respectively, are nearly identical within the experimental error. In contrast to this result we find an about 40% larger peak area of 2.59 mC/cm^2 for the $PtRu(NR_4)$/Vulcan catalyst. We tentatively attribute the reduced active area of the $PtRu(AlR_3)$/Vulcan catalysts as compared to that of the $PtRu(NR_4)$/Vulcan catalyst to the presence of aluminum oxide islands which cover part of the active metal particles on the $PtRu(AlR_3)$/Vulcan catalyst after conditioning and thereby reduce the active surface area available for CO adsorption.

3.3. Potentiodynamic Oxidation of 2% CO/H_2

In order to better simulate the situation in operating fuel cells, where CO/H_2 oxidation occurs under continuous gas flow at a pseudo steady state, we also investigated the potentiodynamic oxidation of 2% CO/H_2 at 60°C (1 mV/s, 2500 rpm) for the unmodified and modified $PtRu(AlR_3)$/Vulcan catalyst. The results are presented in Fig. 4. Prior to the positive-going sweep the potential was held at 0.05 V for about 15 min, until the electrode surface was completely saturated with CO. For comparison current densities of the oxidation of pure hydrogen on the same electrodes at 60°C (10 mV/s, 2500 rpm) are included in the figure (dashed lines). Since the hysteresis was found to be negligible, only the anodic sweep is shown. The hydrogen oxidation reaction is diffusion limited for potentials up to 0.4 V. The diffusion-limited current densities obtained for the supported $PtRu(AlR_3)$/Vulcan catalysts are only about 10% lower than those reported for smooth PtRu alloys (23), which agrees well with previous findings for the $PtRu(NR_4)$/Vulcan catalysts (12). At higher potentials (above about 0.5 V) the current density decreases slightly due to kinetic limitations, which are attributed to surface oxide formation (24). In the presence of 2% CO in H_2 the hydrogen oxidation is completely suppressed up to ≈0.4 V due to CO poisoning of the PtRu surface. At potentials more positive than 0.4 V a sharp increase in current density is observed. For both colloids the theoretical diffusion-limited current density (98% of the current density measured in pure hydrogen) cannot be reached with 2% CO/H_2. We equally attribute this to the oxide-induced decrease in the hydrogen oxidation kinetics at higher potentials mentioned above. The small hysteresis between the anodic and the cathodic sweeps is caused by mass-transport limitations for readsorption of CO on the electrode surface.

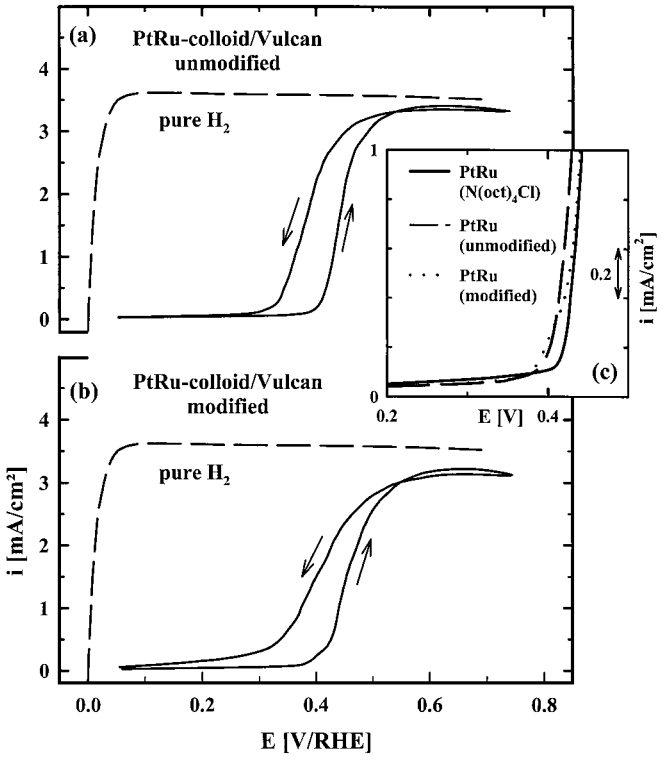

FIG. 4. Potentiodynamic oxidation (1 mV/s) of 2% CO/H_2 at 2500 rpm and 60°C on the unmodified (a) and modified (b) PtRu colloid. The positive-going sweep of the oxidation of pure H_2 is given for reference at 2500 rpm and 60°C. (c) Comparison of the onset for the potentiodynamic (1 mV/s) oxidation of 2% CO/H_2 at 2500 rpm and 60°C in the anodic-going sweep on the unmodified PtRu colloid (---), the modified PtRu colloid (···), and the PtRu colloid/Vulcan from the $N(oct)_4Cl$-stabilized precursor (—). Metal loading in all cases: 7 $\mu g/cm^2$.

For comparison we plotted the onset of the anodic scans of the two $PtRu(AlR_3)$/Vulcan catalysts and also of the $PtRu(NR_4)$/Vulcan catalyst characterized previously (12) in 2% CO in H_2 (1 mV/s, 2500 rpm, 60°C) together in one figure (inset of Fig. 4). The ignition potential for CO/H_2 oxidation (potential where the current density increases by several orders of magnitude in a narrow potential range) is nearly the same for the three PtRu/Vulcan catalysts. It is slightly more negative than that observed on a comparable commercially available PtRu/Vulcan catalyst (E-TEK) (12).

3.4. Potentiostatic Oxidation of Reactant Gas with Lower CO Concentration

Investigations of gas mixtures with 2% CO in H_2 are interesting for examining mechanistic questions or for a comparison of the CO oxidation activity of different anode catalysts. But due to the high anode overpotential (more than 0.4 V) such experiments are irrelevant for performance

predictions of the behavior of state-of-the-art fuel cells. As technical PEMFCs are supposed to work at current densities of 0.5 A/cm^2 with a power density of about 0.3–0.4 W/cm^2 (7), and considering the high kinetic overpotential for the oxygen reduction reaction at the cathode the maximum CO concentrations tolerable are significantly lower. In order to simulate steady-state conditions of real fuel cells we performed similar measurements at lower CO concentrations under potentiostatic conditions (20 min at each potential). Because of the lower CO concentrations and the transport problems associated we allowed longer times for the initial CO poisoning of the electrode surface at 0.015 V (up to 3 h) to reach a fully CO-poisoned electrode surface.

In Fig. 5 we present results of these measurements with 1000 ppm CO/H_2 and 250 ppm CO/H_2 on the unmodified PtRu(AlR_3)/Vulcan catalyst at 60°C and 2500 rpm. Again the oxidation current density for pure hydrogen is plotted for comparison, and for the same reason we also included data on the oxidation of 250 ppm CO/H_2 obtained in RDE measurements on the PtRu(NR_4)/Vulcan catalyst (12) as well as data from real PEMFC measurements (anode, PtRu–E-TEK) (8). In order to simplify the comparison of our results with fuel cell literature the electrode potential is plotted on the ordinate. For the same reason we converted the measured current densities into mass-specific current densities, i_m, which are plotted on the abscissa. (It had been shown previously that mass-specific current densities recorded at comparable metal loadings are the relevant parameter for comparison with fuel cell data (17)).

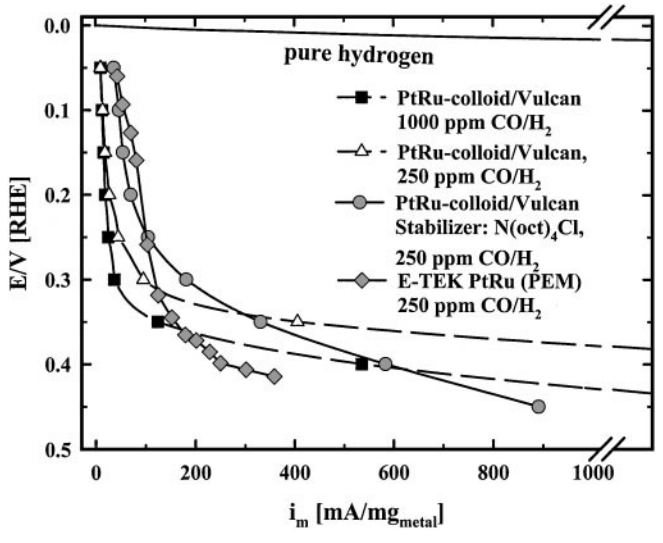

FIG. 5. Potentiostatic oxidation current densities for 1000 ppm CO/H_2 and 250 ppm CO/H_2 (20 min for each potential) on the unmodified PtRu colloid/Vulcan (7 μg of metal/cm^2) at 60°C and 2500 rpm. For comparison the data for 250 ppm CO/H_2 obtained for the PtRu colloid/Vulcan (precursor: N(oct)$_4$Cl-stabilized colloid) at 60°C and for a PtRu–E-TEK gas diffusion electrode in a PEMFC at 65°C (8) are also shown. The abscissa gives the diffusion-corrected current density with respect to the noble metal loading. The current densities for pure hydrogen oxidation are given as a reference.

The mass-specific current density, i_m, given on the abscissa in Fig. 5 is determined from the kinetic current density, i_k, and the metal loading L (here 7 μg of metal/cm^2) via $i_m = i_k/L \cdot i_k$, in turn is extracted from the measured current density, i, via Eq. [2],

$$\frac{1}{i_k} = \frac{1}{i} - \frac{1}{i_d}, \qquad [2]$$

where i_d represents the diffusion-limited current density for the oxidation of pure hydrogen.

For pure hydrogen electrooxidation on the unmodified PtRu(AlR_3)/Vulcan catalyst kinetic limitations are negligible in the current density range between 0 and 1 A/mg of metal. Potentiostatic measurements on the unmodified PtRu(AlR_3)/Vulcan catalyst (Fig. 5) clearly demonstrate that decreasing the CO concentration from 2% to 1000 ppm leads to a decrease of the ignition potential from about 0.4 V (potentiodynamic measurement, inset of Fig. 4) to about 0.35 V. A further decrease of the CO concentration to 250 ppm even reduces the ignition potential to about 0.3 V. Comparing our measurements with data obtained on the PtRu(NR_4)/Vulcan catalyst, also at 250 ppm CO in H_2, we find that the latter one is more active for potentials lower than 0.3 V, whereas at potentials higher than 0.3 V and at fuel cell relevant current densities the PtRu(AlR_3)/Vulcan catalyst is superior.

Comparison of our RDE data with PEM-FC performance data from Divisek *et al.* (8) (250 ppm CO/H_2, 65°C; metal loading, 1.0 mg/cm^2; gray rhomb in Fig. 5) indicates that the electrochemical activity of the PtRu(AlR_3)/Vulcan catalysts is comparable to that of the commercial E-TEK–PtRu catalyst. The good agreement between our RDE data and the fuel cell data also underlines that the thin-film RDE method is a valuable tool for predicting the catalyst performance, or more precisely the kinetic limit of the catalyst performance in a real fuel cell, in the absence of diffusion limitations.

Finally Fig. 5 clearly demonstrates that at current densities of technical interest of about 0.5 A/cm^2 (equivalent to 0.5 A/mg of metal with 1 mg of metal/cm^2) the overpotential between oxidation of pure H_2 and that of a gas mixture of 250 ppm CO in H_2 is still about 0.3 V. Hence, the CO tolerance of the characterized catalyst at 60°C is still far below 250 ppm CO. A more quantitative estimate can be made by using the PEM single-cell measurements by Oetjen *et al.* (25) and by Divisek *et al.* (8) (20 wt% $Pt_{0.5}Ru_{0.5}$/Vulcan catalyst, 1 mg of PtRu/cm^2). According to their measurements the difference in cell potentials between using pure H_2 and a mixture of 50 ppm CO in H_2 amounts to about 150 mV, and for 25 ppm CO in H_2 to about 80 mV. Defining the CO tolerance as the maximum concentration of CO in H_2 where the anode polarization with respect to pure H_2

does not exceed 50 mV, the CO tolerance for PtRu anode catalysts at 80°C must clearly be below 25 ppm.

While PtRu is generally considered as the "state-of-the-art" anode catalyst for reformate-operated PEM fuel cells, there is still potential for improvement, as evidenced by comparing its CO tolerance with those of other Pt metal alloy catalysts. A recent RDE study on the activity of carbon-supported $Pd_{0.8}Au_{0.2}$ catalysts for H_2/CO electrooxidation showed this to be about 4 to 6 times more active in a H_2/CO saturated electrolyte with 250 ppm CO for potentials below 300 mV (26). At current densities of 0.5 A/cm^2 both catalysts behave nearly identically. Investigations on carbon-supported Pt_3Sn catalysts revealed an overpotential of about 230 mV between the oxidation of pure H_2 and a mixture of 250 ppm CO in H_2 at a current density of 0.5 A/cm (27). Compared to the overpotential of 300 mV found for the PtRu catalysts investigated here, the anode polarization is clearly diminished. It has to be proven, however, that these superior values also hold true for (technically relevant) lower CO concentrations, which are not accessible in open-cell RDE measurements because of the very long times required for equilibration, and whether these catalysts are compatible with PtRu with respect to its long-term stability.

3.5. Potentiostatic Methanol Electrooxidation

In the last section we focus on the activity of the modified and unmodified PtRu(AlR_3)/Vulcan catalysts towards methanol oxidation. Figure 6 summarizes the resulting activities obtained from potentiostatic stepping experiments at 60°C, measured 30 min after stepping the potential into the range between 0.4 and 0.55 V. For comparison we again include similar data obtained on the PtRu(NR_4)/Vulcan catalyst (13) and on a commercial PtRu/Vulcan catalyst (E-TEK).

First the modified and the unmodified PtRu(AlR_3)-Vulcan catalysts show a very similar performance for electrooxidation of 0.5 M methanol. Their activity, however, is less than that of the PtRu(NR_4)/Vulcan catalyst at all potentials examined, by 25–50%, despite the lower dispersion of the latter catalyst (particle sizes are listed in Table 1). Finally, compared to the performance of the commercial Pt/Vulcan (E-TEK) catalyst, the three colloid-based PtRu catalysts turn out to be superior for potentials below 0.55 V (13).

The higher activity of the PtRu(NR_4)/Vulcan catalyst cannot be explained in a simple way at this point. It may be related to a higher amount of (111) microfacets on the larger particles of the latter catalyst, since according to Chrzanowski *et al.* the Pt(111)/Ru surface is more active than those of Pt(100)/Ru, Pt(110)/Ru, and Pt(poly)/Ru (28, 29). Another possibility involves effects caused by the presence of the aluminum oxide on the particle surface, which may affect methanol oxidation more than CO oxidation. A more definite answer, however, demands further investigation.

The better performance of PtRu alloy catalysts compared to a pure Pt catalyst over a wide potential range is generally explained by the higher affinity of the Ru surface atoms

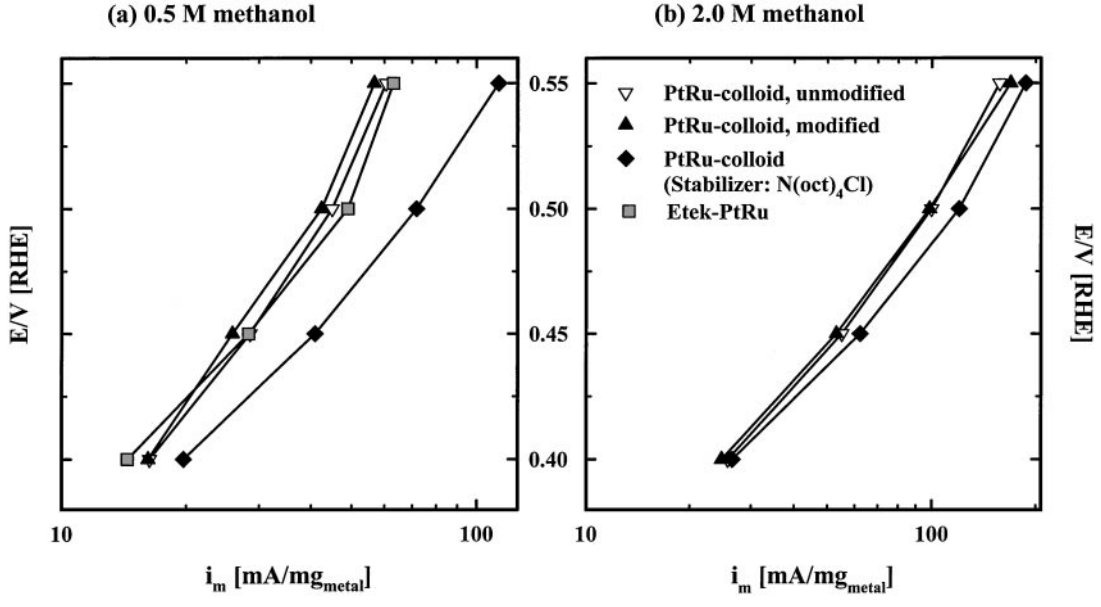

FIG. 6. Electrooxidation of (a) 0.5 M methanol and (b) 2.0 M methanol: comparison of the mass-specific current densities on the unmodified and modified PtRu colloid, the PtRu colloid from the N(oct)$_4$Cl-stabilized precursor, and E-TEK–PtRu. Conditions: 0.5 M H_2SO_4, 60°C, 30 min for each potential.

toward OH formation, which makes it possible to generate the OH_{ad} required for the oxidation of the CO that is formed as reaction intermediate during methanol oxidation at more cathodic potentials than on Pt, at ~0.35 V instead of >0.55 V (30). It should be noted, however, that good catalysts for the electrooxidation of CO are not necessarily good catalysts for methanol electrooxidation (27). At potentials higher than about 0.55 V pure Pt becomes more active than PtRu (31). Potentials higher than 0.55 V, however, are irrelevant for DMFC applications where the anode potential is held at about 0.4 V. The higher activity of pure Pt at higher potentials can be explained on the basis of the formation of strongly bonded surface oxide at lower potentials on Ru than on Pt (30), which blocks either the dissociative adsorption of methanol or reduce the kinetics of CO_{ad} oxidation.

Going to a higher methanol concentration of 2.0 M we found little change in the oxidation behavior of the three PtRu colloid-based catalysts. The measured oxidation currents for the unmodified as well as for the modified $PtRu(AlR_3)$/Vulcan catalysts are between 1.5 (0.4 V) and 3.0 (0.55 V) times higher for the reaction in 2.0 M methanol than in 0.5 M methanol, which can be understood from the higher equilibrium surface coverage of methanol or methanol dehydrogenation fragments when going to higher methanol concentrations. These findings are in good agreement with results on the interdependence between current and methanol concentration obtained on smooth PtRu electrodes (32). A similar behavior of the current density versus methanol concentration was reported also for platinized Pt electrodes for methanol concentrations up to about 1.0 M methanol (33).

The electrocatalytic activity of the $PtRu(AlR_3)$/Vulcan catalysts for the oxidation of 0.5 M and 2.0 M methanol compares well not only with the PtRu catalyst from E-TEK, but also with other state-of-the-art PtRu electrocatalysts prepared via traditional routes (e.g., Refs. (9, 34, 35)). These results clearly demonstrate that the colloid-based PtRu catalysts, both the unmodified and modified $PtRu(AlR_3)$/Vulcan as well as the $PtRu(NR_4)$/Vulcan catalyst, are not only promising candidates for the oxidation of CO contaminated H_2, but also have a high potential as catalysts for the methanol oxidation reaction.

Finally it should be noted that despite the very good performance of the colloid-based catalysts, at least relative to the state-of-the-art catalysts, significant improvements are still required, as is evident from a simple estimate. If we assume a cathode potential of 0.8 V and an anode potential of 0.45 V, our cell potential amounts to 0.35 V and the current density obtained in 2.0 M methanol is about 50 mA/mg of metal. We therefore reach a mass-specific power of about 20 mW/mg of metal. At this activity it would take about 2.6 kg of noble metal to generate the 50 kW planned for fuel cell-operated electrovehicles. Hence there is still an urgent need for further catalyst improvement to lower the amount of noble metal.

4. CONCLUSION

We demonstrated that a new, less complex and hence less costly route for the synthesis of surfactant-stabilized PtRu colloids can be used to prepare highly active PtRu catalysts for electrooxidation of CO-contaminated H_2 and of methanol in PEM-FC and DMFC anodes, respectively. The synthesis is simplified by using aluminum organic compounds as both reducing agent and stabilizer. Furthermore, these stabilized colloids can easily be converted into a more hydrophilic form, which simplifies the further handling of the colloid. Based on microscopic and spectroscopic measurements, by TEM/EDX and XPS, performed at different stages of the supporting and conditioning process, respectively, a conditioning procedure was worked out which combines complete removal of the aluminum organic stabilizer shell and insignificant sintering. Oxidation and subsequent reduction at 250°C or 300°C, for the unmodified and the modified colloids, respectively, lead to metallic PtRu particles of 1.5 ± 0.4 nm and 1.8 ± 0.5 nm average particle size.

Using RDE measurements we could prove that the Vulcan-supported conditioned catalysts obtained from the above-described colloids show activity toward oxidation of 2% CO/H_2 and 0.5 or 2.0 M methanol comparable to that of the catalyst obtained from $PtRuN(oct)_4Cl$ or a commercially available PtRu catalyst.

The relatively high activity and CO tolerance of the colloid-based PtRu catalysts achieved already without extensive optimization, in conjunction with the significant improvements in the synthesis and handling of the colloid precursor reported in this study and the high potential for further controlled modification of particle size, make these catalysts an attractive alternative for multicomponent catalysts prepared along traditional routes.

Nevertheless, the presented synthesis route is still complex and expensive compared to the state-of-the-art coimpregnation method. Additionally the influence of the remaining Al needs further investigation. Despite these restrictions this synthesis methods is of great importance in catalyst research and development.

Finally this study provides further proof that mass-specific H_2 current densities determined via RDE measurements are consistent with the current densities reported from PEM fuel cell measurements, in the absence of transport limitations, and hence can be used as a simple tool for predictions of the kinetic limit for the performance of catalysts in a real fuel cell.

ACKNOWLEDGMENTS

We thank A. Rämisch and K. Kraft for the glass cells and the express repairs. Furthermore, we acknowledge E-TEK (J. Giallombardo) and

Degussa AG as well as Hochtemperatur Werkstoffe GmbH for the donation of the catalyst, platinum wire, and glassy carbon substrates, respectively. Financial support for this work came from the Deutsche Forschungsgemeinschaft (Projekt BE 1201/8-1, BO 1135/2-1), the Fonds der Chemischen Industrie, and the Ulmer Universitätsgesellschaft.

REFERENCES

1. Bönnemann, H., Brijoux, W., Brinkmann, R., Dinjus, E., Joussen, T., and Korall, B., *Angew. Chem.* **103**, 1344 (1991).
2. Bönnemann, H., and Brijoux, W., *in* "Active Metals" (A. Fürstner, Ed.), p. 339. VCH, Weinheim, 1995.
3. Bönnemann, H., Braun, G., Brijoux, W., Brinkmann, R., Schulze-Tilling, A., Seevogel, K., and Siepen, K., *J. Organomet. Chem.* **520**, 143 (1996).
4. Reetz, M. T., Quaiser, S., Breinbauer, R., and Tesche, B., *Angew. Chem.* **107**, 2956 (1995).
5. Schmid, G., Lehnert, A., Kreibig, U., Adamczyk, Z., and Belouschek, P., *Z. Naturforsch.* **456**, 989 (1990).
6. Schmid, G., "Colloids and Clusters." VCH, Weinheim, 1996.
7. Schmidt, V. M., Ianello, R., Oetjen, H.-F., Reger, H., Stimming, U., and Trilla, F., *in* "Proceedings of the First International Symposium on Proton Conducting Membrane Fuel Cells I" (S. Gottesfeld, G. Halpert, and A. R. Landgrebe, Eds.), ECS Conf. Proc. 95-23, pp. 267–277. The Electrochemical Society, Pennington, NJ, 1995.
8. Divisek, J., Oetjen, H.-F., Peinecke, V., Schmidt, V. M., and Stimming, U., *Electrochim. Acta* **43**, 3811 (1998).
9. Cameron, D. S., Hards, G. A., and Thompsett, D., *in* "Direct Methanol Fuel Cells" (A. R. Landgrebe, R. K. Sen, and D. J. Wheeler, Eds.), ECS Conf. Proc. 92-14, pp. 12–23. The Electrochemical Society, Pennington, NJ, 1992.
10. Schmidt, V. M., Ianello, R., Oetjen, H.-F., Reger, H., and Stimming, U., *in* "Proceedings of the First International Symposium on Proton Conducting Membrane Fuel Cells I" (S. Gottesfeld, G. Halpert, and A. R. Landgrebe, Eds.), ECS Conf. Proc. 95-23, pp. 1–11. The Electrochemical Society, Pennington, NJ, 1995.
11. Schmidt, T. J., Noeske, M., Gasteiger, H. A., Behm, R. J., Britz, P., Brijoux, W., and Bönnemann, H., *Langmuir* **13**, 2591 (1997).
12. Schmidt, T. J., Noeske, M., Gasteiger, H. A., Behm, R. J., Britz, P., Brijoux, W., and Bönnemann, H., *J. Electrochem. Soc.* **145**, 925 (1998).
13. Schmidt, T. J., Gasteiger, H. A., and Behm, R. J., *Electrochem. Commun.* **1**, 1 (1999).
14. Götz, M., and Wendt, H., *Electrochim. Acta* **43**, 3637 (1998).
15. Bönnemann, H., Brinkmann, R., Britz, P., Endruschat, U., Mörtel, R., Paulus, U., Feldmeyer, G., Schmidt, T. J., Gasteiger, H. A., and Behm, R. J., *J. New Mater. Electrochem. Syst.* **3**, 199 (2000).
16. Schmidt, T. J., Gasteiger, H. A., Stäb, G. D., Urban, P. M., Kolb, D. M., and Behm, R. J., *J. Electrochem. Soc.* **145**, 2354 (1998).
17. Schmidt, T. J., Gasteiger, H. A., and Behm, R. J., *J. Electrochem. Soc.* **146**, 1296 (1999).
18. Denton, J., Gascoyne, J. M., and Thompsett, D., European Patent EP 0 731 520 A1, 1996.
19. Hadzi-Jordanov, S., Angerstein-Kozlowska, H., Vukovic, M., and Conway, B. E., *J. Electrochem. Soc.* **125**, 1471 (1978).
20. Gasteiger, H. A., Markovic, N., Ross, P. N., and Cairns, E. J., *J. Phys. Chem.* **98**, 617 (1994).
21. Iwase, M., and Kawatsu, S., *in* "Proceedings of the First International Symposium on Proton Conducting Membrane Fuel Cells I" (S. Gottesfeld, G. Halpert, and A. R. Landgrebe, Eds.), ECS Conf. Proc. 95-23, pp. 12–23. The Electrochemical Society, Pennington, NJ, 1995.
22. Starz, K. A., Auer, E., Lehmann, T., and Zuber, R., Presented at the 6th Grove Fuel Cell Symposium, London, 1999.
23. Gasteiger, H. A., Markovic, N. M., and Ross, P. N., *J. Phys. Chem.* **99**, 8290 (1995).
24. Vielstich, W., "Fuel Cells." Wiley-Interscience, London, 1970.
25. Oetjen, H.-F., Schmidt, V. M., Stimming, U., and Trila, F., *J. Electrochem. Soc.* **143**, 3838 (1996).
26. Schmidt, T. J., Ph.D. Dissertation, Univ. Ulm, 2000.
27. Schmidt, T. J., Gasteiger, H. A., and Behm, R. J., *in* "Elektrochemische Reaktionstechnik und Synthese—Von den Grundlagen bis zur industriellen Anwendung" (J. Russow, G. Sandstede, and H. Staab, Eds.), Vol. 14, p. 196. GDCh, Frankfurt, 1999.
28. Chrzanowski, W., and Wieckowski, A., *Langmuir* **14**, 1967 (1998).
29. Chrzanowski, W., Kim, H., and Wieckowski, A., *Catal. Lett.* **50**, 69 (1998).
30. Kinoshita, K., "Electrochemical Oxygen Technology." Wiley, New York, 1992.
31. Gasteiger, H. A., Markovic, N., Ross, P. N., and Cairns, E. J., *J. Electrochem. Soc.* **141**, 1795 (1994).
32. Chu, D., and Gilman, S., *J. Electrochem. Soc.* **143**, 1685 (1996).
33. Bagotzky, V. S., and Vassilyev, Y. B., *Electrochim. Acta* **12**, 1323 (1967).
34. Watanabe, M., Uchida, M., and Motoo, S., *J. Electroanal. Chem.* **229**, 395 (1987).
35. Hamnett, A., Weeks, S. A., Kennedy, B. J., Troughton, G., and Christensen, P. A., *Ber. Bunsenges. Phys. Chem.* **94**, 1014 (1990).